3D Flow of Deposits on the Surface of Cathode Blocks in an Aluminium Electrolysis Cell

Marc LeBreux[1], Aimen E. Gheribi[2], Martin Désilets[3], Gervais Soucy[4], Patrice Chartrand[5], Patrick Pelletier[6], Jean-François Bilodeau[7] and Didier Lombard[8]

1. Research assistant

Faculté de génie, Université de Sherbrooke, Sherbrooke (Québec) Canada J1K 2R1

2. Research assistant

École Polytechnique de Montréal, Montréal (Québec) Canada H3T 1J4

3. Professor

4. Professor

Faculté de génie, Université de Sherbrooke, Sherbrooke (Québec) Canada J1K 2R1

5. Professor

École Polytechnique de Montréal, Montréal (Québec) Canada H3T 1J4

6. Research scientist- lining

7. Coordinator, Reduction cell modeling and design

CRDA Électrolyse, RioTinto, Saguenay (Québec) Canada G7S 4K8

8. Innovation champion & Material expert- lining

LRF, RioTinto, Saint-Jean-de-Maurienne France 73302

Corresponding author: gervais.soucy@usherbrooke.ca

Abstract

Lab-scale experiments and observations from industrial aluminum electrolysis cells have shown that a layer of deposits can be formed at the surface of the cathode blocks. Studies have shown that the thickness, composition and state (liquid, mushy, solid) of the deposits can vary along the cathode surface, depending on the operational conditions. The deposits are highly resistive and at the origin of local horizontal currents generated in the cell, a situation that is not favorable to cell stability. Moreover, these deposits increase the cathode voltage drop (CVD) which also reduces the energy efficiency of the cells. When they are in the liquid state, these deposits have been suggested to be the source for the back feeding and for ledge formation at the metal level. Some authors have postulated that at the metal level, the formation of the ledge is only possible if there exist a bath film between the metal and the ledge. In order to understand more clearly the behavior of the deposits at the surface of the cathode, a transient multiphase finite-volume model is developed to couple the mass and momentum conservation equations to a hybrid method combining the volume of fluid and level-set function. The numerical model enables to predict the time-varying velocity field and volume fraction of the deposits. From these predictions, the mass flow of deposits moving along the cathode surface is calculated and compared to values reported in the open literature. The proposed model is finally used to verify the impact of the initial deposit thickness on the movement of deposits and the corresponding mass flow. For a cathodic panel periphery of 30 m long, results show that the mass flow of the deposits vary over time, with a rapid initial peak and then an exponential decrease ending up to a value two orders of magnitude smaller than the peak. For an initial thickness of 0.5 mm and 1.5 mm, the calculated final thicknesses are respectively 0.25 mm and 0.4 mm, while the mass flow peak values are 0.17 - 0.19 kg/s and 0.55 - 0.76 kg/s.

Keywords: Aluminum electrolysis cell, bottom deposits, mathematical modeling, CFD, multiphase flow.

1. Introduction

Lab-scale experiments and observations from industrial aluminum electrolysis cells have shown that a layer of deposits can be formed at the surface of the cathode blocks [1 - 6]. As reported in these studies, the deposits consist of a mixture of electrolytic bath and alumina. Results have shown that the thickness, composition and state (liquid, mushy, solid) of the deposits can vary along the cathode surface, depending on the operational conditions (Figure 1). The deposits are highly resistive and can lead to local horizontal currents, a situation that is not favorable to cell stability. Moreover, these deposits increase the cathode voltage drop (CVD) which also reduces the energy efficiency of the cells.

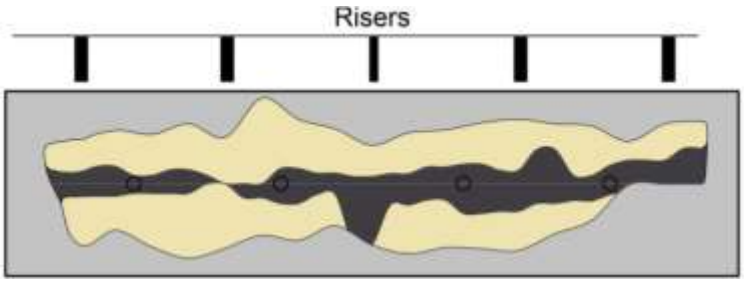

a) Schematic top view of the deposits formation [3]: Grey zone- ledge toe, Yellow zone- thin film, Dark zone – thick deposits

b) Surface of industrial cathode block [4]

Figure 1. Deposits on the surface of cathode blocks.

In addition, when the deposits are in the liquid state, they have been suggested to be one of the mechanisms for the back feeding and ledge formation at the metal level. The ledge at this location behaves differently than at the bath level as reported in various studies [7 - 9]. Some authors have postulated that at the metal level, the formation of the ledge is only possible if there exist a bath film between the metal and the ledge.

For years, numerical modeling of aluminum electrolysis cells has been performed and enabled to achieve more energy efficient aluminum production [10]. In the current work, a transient finite-volume numerical model is first developed in order to understand more clearly the behavior of the deposits at the surface of the cathode. The model enables to predict the time-varying velocity field and volume fraction of the deposits. From this information, the objective is to gain knowledge on the deposits mass transfer process in the optics of later adjusting the operational parameters of the electrolysis cell or to modify the design of cathode blocks so to minimize the impact of resistive deposits on its surface.

From the time-varying velocity field and volume fraction of the deposits, the current work aims secondly to predict the mass flow of deposits moving along inclined geometry of cathode blocks and to compare it with values reported in the open literature. Finally, the proposed model is used to verify the impact of the initial deposits thickness on its movement and the corresponding mass flow.

2. Presentation of the Numerical Model

The problem under investigation is depicted in Figure 2. Three immiscible liquid phases are considered in this study: 1) metal, 2) deposits, and 3) pseudo-carbon. As described in the assumptions, the solid carbonaceous cathodic block is considered as a very viscous liquid to be able to consider the interfacial forces between this surface and the two other liquids. The three phases are initially located in the configuration shown in Figure 2 a). Because the deposits can, in certain conditions, be less dense than the metal [11], they will start moving due to hydrostatic pressure from the metal combined to surface tension effects between the different phases. In order to understand more clearly the behavior of the deposits at the surface of the cathode, a numerical model is developed. It consists of a transient multiphase finite-volume model coupling the mass and momentum conservation equations to a hybrid method combining the volume of fluid and level-set function. From the initial configuration of Figure 2 a), the numerical model enables to predict the time-varying velocity field and volume fraction of each of the phases. Boundary conditions shown in Figure 2 c) will be described later in this section.

The geometry under investigation is not representative of the dimensions of real industrial cathode blocks. The choice to use a small-scale model enables to obtain a reasonable calculation time with the computer resources available and gives the possibility to conduct sensitivity analyses. Still it is necessary to understand more clearly at a lower scale how the thin deposits behave when they are affected by the gravitational and surface tension forces.

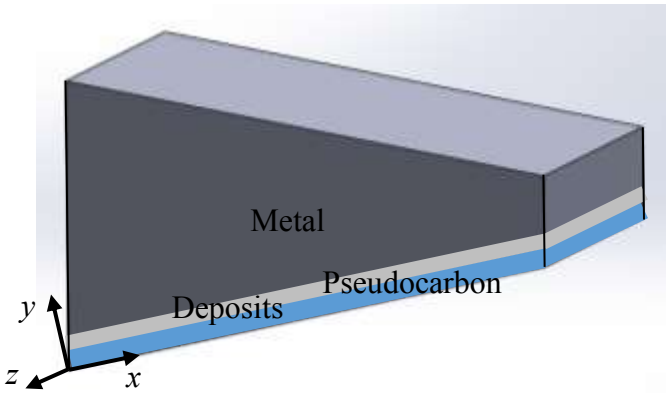

a) Three liquid phases at initial time

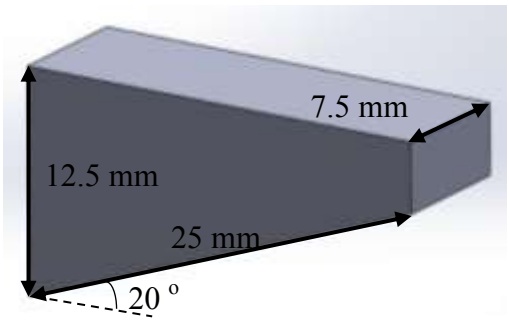

b) Dimensions

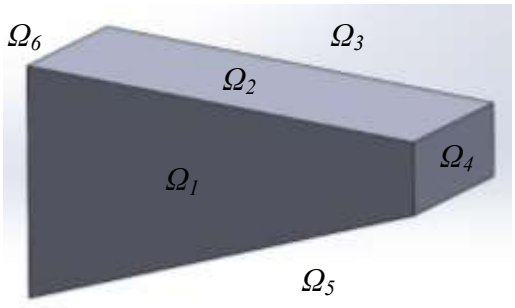

c) Boundaries

Figure 2. Schematics of the geometry under investigation.

In order to track accurately the interface between the different phases, the volume of fluid method is coupled to the level-set method, which is a popular interface-tracking method for computing multiphase flow with complex interfaces. In the level-set method, the interface is represented by the zero contour of a continuous signed distance function known as the level-set

function. The movement of the interface is governed by a transport equation for the level set function [12]. Because the level-set function is smooth and continuous, its spatial gradients can be accurately calculated, which will in turn produce accurate estimates of interface curvature and surface tension force caused by the curvature. However, the level-set method is found to have a deficiency in preserving volume conservation. On the other hand, the volume of fluid method is naturally volume-conserved, as it computes and tracks the volume fraction of a particular phase in each cell rather than the interface itself. The weakness of the volume of fluid method lies in the calculation of its spatial derivatives and thus affecting the surface tension force caused by the curvature. To overcome the deficiencies of both the level-set method and the volume of fluid method, a coupled approach between these two methods is employed [13].

The mathematical model for solving this transient problem rests on the following assumptions:

- No heat transfer is considered
- No metal movement from MHD effects is taken into account, the metal is moving only due to gravity and surface tension effects
- In this configuration, the flow of the liquid phases is considered laminar
- The liquid phases are considered incompressible fluids
- The properties of the individual phases are perfectly known
- The deposits are composed of pure electrolytic bath
- The pseudo-carbon, a really viscous liquid layer, denser than metal, mimics the solid cathode surface and enables to specify surface tension coefficient along the interface between each pair of phases.

Both level set and volume of fluid methods are known as "one" fluid methods, where a single set of conservation equations is solved and the interface is captured via a scalar function. The level-set function is used to compute the surface tension contribution to the momentum equations, via curvature and its normal to the interface while the volume of fluid function is used to capture the interface itself [12, 13]. Based on the foregoing assumptions, the governing conservation equations for mass, momentum, and level-set function are stated as:

$$\frac{\partial \rho}{\partial t} + \nabla \cdot \left(\rho \vec{V}\right) = 0 \tag{1}$$

$$\frac{\partial}{\partial t}\left(\rho \vec{V}\right) + \nabla \cdot \left(\rho \vec{V}\vec{V}\right) = -\nabla p + \nabla \cdot \left[\mu\left(\nabla \vec{V} + \nabla \vec{V}^{T}\right)\right] + \rho \vec{g} - \vec{F}_{st} \tag{2}$$

$$\frac{\partial \varphi}{\partial t} + \nabla \cdot \left(\varphi \vec{V}\right) = 0 \tag{3}$$

where:

ρ	Density, kg/m^3
t	Time, s
$\vec{V}$	Velocity field, m/s
p	Static pressure, Pa
μ	Dynamic viscosity, kg/m.s
$\vec{g}$	Gravitational acceleration, m/s^2
$\vec{F}_{st}$	Body force arising from surface tension effects, N/m^3
φ	Level-set function

The conservation of φ in Equation (3) does not guarantee that the mass enclosed by φ is conserved [14]. Level-set methods are known to suffer from errors in mass conservation; therefore, the level-set must be reinitialized every time step to reduce errors in the resolution of the interface. In the reinitialization process, the volume of fluid method provides the volume of

each fluid present in a cell, and the level-set function determines the orientation of the interface between fluids [13]. As a result, surface effects are calculated more accurately and mass is conserved [15].

In the above conservation equations, the density ρ and viscosity μ are calculated from the level-set function and the individual properties of the phases presented in Table 1. As presented in Equation (2), the numerical model includes the effect of surface tension along the interface through the specific force $\vec{F}_{st}$. This term is approximated using the continuum surface force (CSF) model of Brackbill [17]. In order to compute this term, the surface tension coefficient between each pair of phases are presented in Table 2.

The boundary conditions applied on the set of partial derivatives equations are presented in Table 3 where the boundaries are shown in Figure 2 c). They consist of null speed (wall condition) or null gradient of speed (symmetry condition).

Table 1. Properties of each phases [7, 16].

Phase	Density (kg/m^3)	Viscosity (kg/m.s)
Metal	2300	0.00138
Deposits	2080	0.0024
Pseudocarbon	2400	1

Table 2. Surface tension coefficient between each pair of phases [18].

Phases	Surface tension coefficient (N/m)
Metal/Deposits	0.55
Metal/Pseudocarbon	10
Deposits/Pseudocarbon	0

Table 3. Boundary conditions.

Boundary	Condition	Mathematical formulation
Ω_1	Symmetry	$\frac{d\vec{V}}{d\vec{n}} = 0$
Ω_2	Symmetry	$\frac{d\vec{V}}{d\vec{n}} = 0$
Ω_3	Symmetry	$\frac{d\vec{V}}{d\vec{n}} = 0$
Ω_4	Wall	$\vec{V} = 0$
Ω_5	Wall	$\vec{V} = 0$
Ω_6	Wall	$\vec{V} = 0$

Regarding the initial conditions, the velocity field is null throughout the geometry, so there is no movement from any phases:

$$\vec{V}(x, y, z, t = 0) = 0 \quad (4)$$

As for the initial volume fraction of each phases, they are presented in Figure 3. In this study, two different cases are considered: case #1 where the initial thickness of deposits is 0.5 mm, and case #2 where the initial thickness of deposits is 1.5 mm. In each case, the thickness of the pseudo-carbon layer is taken as 1 mm, while the metal phase takes on the remaining space inside the geometry.

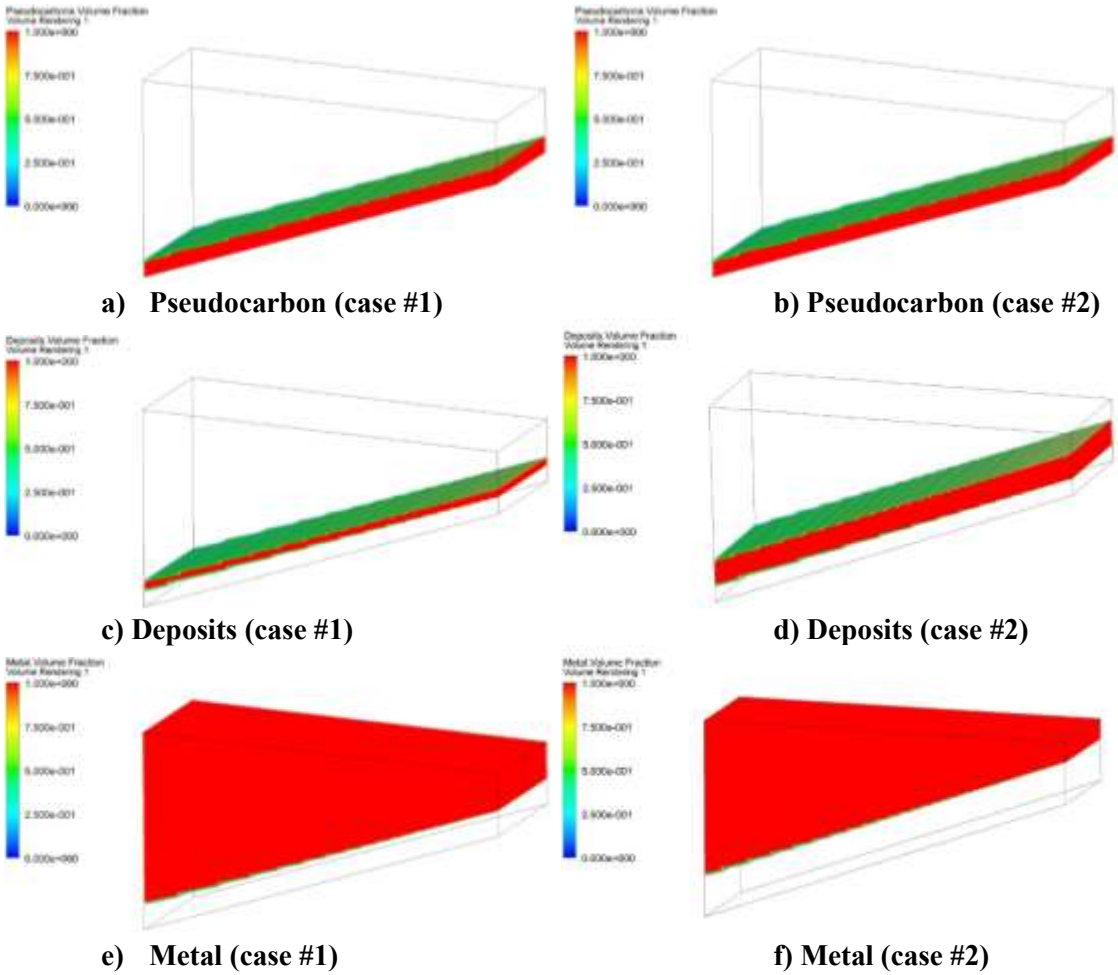

a) Pseudocarbon (case #1) b) Pseudocarbon (case #2)

c) Deposits (case #1) d) Deposits (case #2)

e) Metal (case #1) f) Metal (case #2)

Figure 3. Representation of initial volume fraction of each phases used for two different cases (case #1 and case #2).

From the geometry under investigation (Figure 2), the three liquid phases with their corresponding properties (Tables 1 - 2), the boundary conditions (Table 3), and initial conditions (Equation 5, Figure 3), Equations (1)-(3) are discretized using finite-volumes. A total of 697 200 hexahedral finite-volumes of dimensions 0.15 mm x 0.15 mm x 0.15 mm, composed 20 nodes, are used in the numerical model for a total of 2 868 733 nodes. In this study, the pressure-velocity coupling is performed using the pressure implicit with split of operators (PISO) scheme with a coupled Skewness-Neighbor correction. The volume of fluid method is discretized using the explicit formulation. The spatial discretization of the pressure, momentum, volume fraction, and level-set functions are respectively performed with the body force weighted formulation, the second order upwind scheme, the compressive scheme, and first order upwind scheme. The first order implicit time scheme are used to discretize the time derivative in the conservation equations.

For each time step, a coupled set of algebraic equations are then solved iteratively using ANSYS Fluent [13] until the conservation equations residuals fall below a small value. The time step and number of time steps used in the present model are respectively 0.0001 s and 40 000 which corresponds to a total simulation time of 4 s. Using an Intel ® Xeon ® Quad CPU E5-1620 3.6 GHz computer that possess 8 GB of RAM, a computer easily available, the number of nodes and the value of the time step were chosen as a compromise between calculation time and numerical accuracy. The numerical model can thus provide the time-varying velocity field and volume fraction of each of the phases.

3. Results

The proposed numerical model is now used to verify the impact of the initial deposit thickness on both the dynamic behavior of the deposits and the corresponding mass flow of deposits generated along an inclined geometry mimicking the carbon paste slope on the side of electrolysis cells. As reported in Figure 3 b), initial deposits thickness of 0.5 mm and 1.5 mm are under investigation.

For the deposits of 0.5 mm, the evolution over time of the deposits volume fraction is first presented in Figure 4. Results show the change in the deposits thickness from its initial profile. One can observe the battle between the gravitational and surface tension forces. A portion of the deposits, less dense than the metal, will form bubbles that will rise through the metal and accumulates above it. In this case, the hydrostatic pressure from the metal is lower than the force generated from tension surface effects, and the bubbles can form. However, as shown in Figure 4, a certain portion of the deposits remains at the bottom, attached to the pseudo-carbon layer. In this case, the hydrostatic pressure from the metal is higher than the surface tension force, which hinder the removal of the deposits from the cathode surface.

The results for deposits of 1.5 mm thick are next presented in Figure 5. Results show once again the change in the deposits thickness from its initial profile. Once again, a portion of the deposits will go above the metal, and one portion of the deposits will stick at the bottom, attached to the pseudo-carbon layer. Because the initial thickness of the deposits is larger in this case, Figure 5 show that initially there is a stronger mixing of the phases.

From the time-varying velocity field and the volume fraction of deposits, the mass flow of deposits flowing along the inclined geometry, just above the pseudo-carbon layer, is calculated. Because the width of the geometry under investigation is only 7.5 mm, the mass flow rate estimation is corrected for a real industrial cell geometry, i.e. for a cathodic panel periphery of 30 m long. Referring to Figure 2, the mass flow calculations are performed at three locations on the x axis: $x = 0.007$ m, $x = 0.01$ m, and $x = 0.013$ m. The results for both cases are presented in Figure 6.

For each of the locations chosen in the x direction, results show that the mass flow of the deposits varies over time, with a rapid initial peak and then an exponential decrease ending up to a value two orders of magnitude smaller than the peak. For the case where the deposits have an initial thickness of 1.5 mm, the mass flow of deposits follow the same trend. However, in this case, the peak value is larger, and the deposits seem to take more time to attain this initial peak.

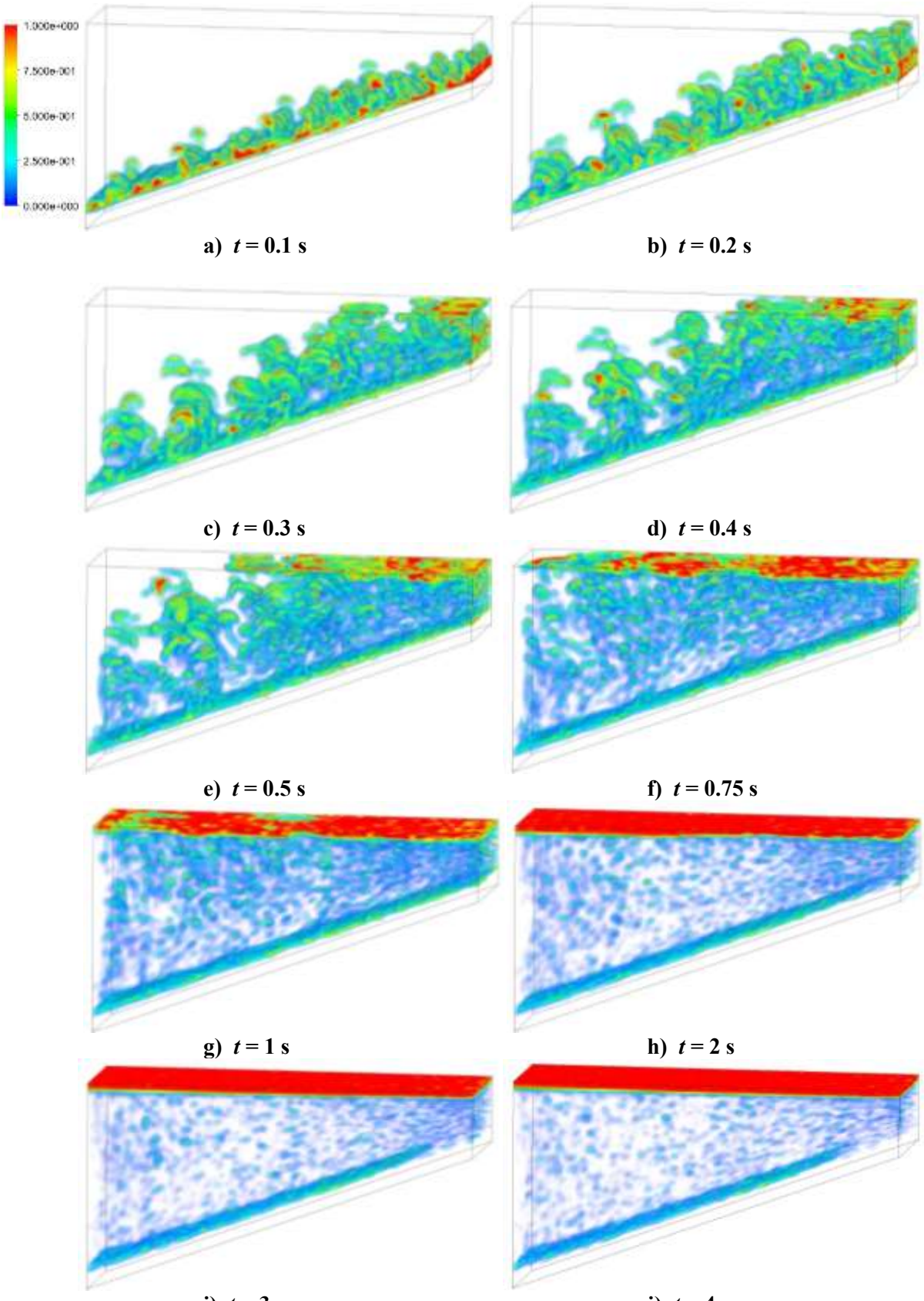

a) $t = 0.1$ **s** **b)** $t = 0.2$ **s**

c) $t = 0.3$ **s** **d)** $t = 0.4$ **s**

e) $t = 0.5$ **s** **f)** $t = 0.75$ **s**

g) $t = 1$ **s** **h)** $t = 2$ **s**

i) $t = 3$ **s** **j)** $t = 4$ **s**

Figure 4. Simulated volume fraction of the deposits formed on the top of the cathode material – The initial thickness of deposits is 0.5 mm.

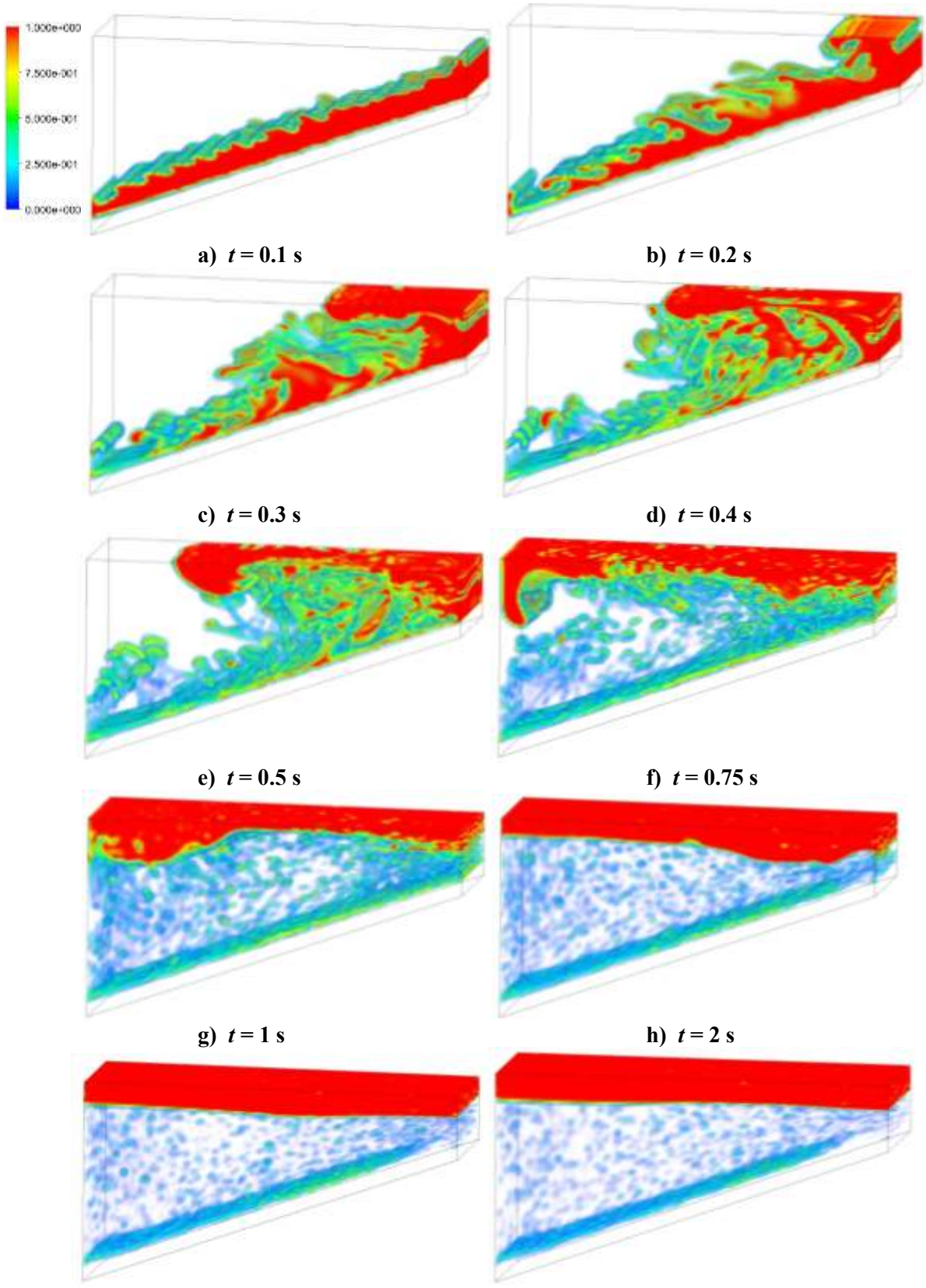

a) $t = 0.1$ s **b)** $t = 0.2$ s

c) $t = 0.3$ s **d)** $t = 0.4$ s

e) $t = 0.5$ s **f)** $t = 0.75$ s

g) $t = 1$ s **h)** $t = 2$ s

i) $t = 3$ s **j)** $t = 4$ s

Figure 5. Simulated volume fraction of the deposits formed on the top of the cathode material – The initial thickness of deposits is 1.5 mm.

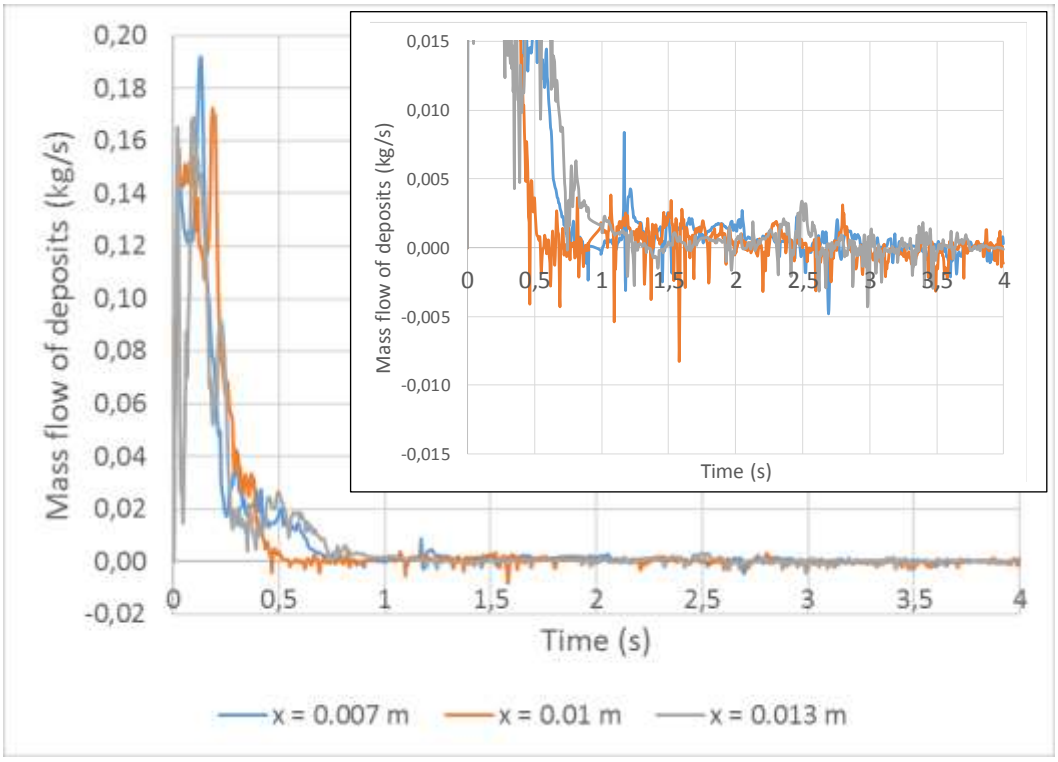

a) Simulated mass flow of the deposits formed on the top of the cathode material with an initial thickness of 0.5 mm.

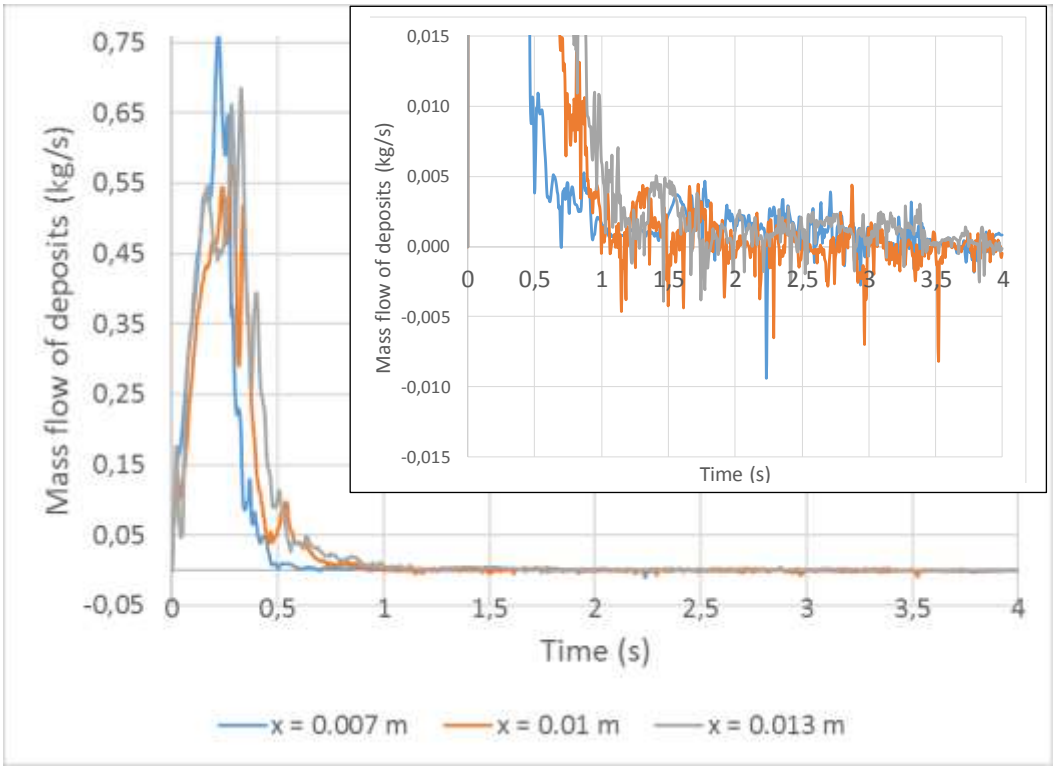

b) Simulated mass flow of the deposits formed on the top of the cathode material with an initial thickness of 1.5 mm.

Figure 6. Simulated mass flow of deposits formed on the top of cathode material corrected for a complete industrial cell.

The calculated values for the mass flow of deposits are now compared with values reported in the open literature [7, 19]. In reference [7], the author developed an analytical 1D model based

on a simplified Navier-Stokes equation in order to relate the deposits thickness to its the mass flow flowing along the inclined sideledge:

$$\dot{m} \quad \text{———} \qquad (5)$$

where:

$\dot{m}$ Mass flow of deposits, kg/s
Density of deposits, kg/m^3
Difference of density between the metal and deposits phases, kg/m^3
Gravitational acceleration in the flow direction, m/s^2
Deposits thickness, m
L Length of sideledge periphery, m
Dynamic viscosity of deposits, kg/m.s

Equation (5) assumes that the bath film between the metal and sideledge is based on a source of liquid at the cell bottom. As reported in reference [7], other mechanisms, which are not taken into account by Equation (5), may also contribute to the dynamic behavior of the bath film.

The mass flow of deposits is estimated for different angles, using Equation (5) and known values of deposits thickness (0.2 mm and 0.5 mm) obtained from autopsies performed on dead electrolysis cells [4]. For these calculations, the properties of the metal and deposits are taken from Table 1, and the length of sideledge periphery L = 30 m is chosen to be equal to the length of the cathodic panel periphery. The results, presented in Figure 7, show that the calculated mass flow varies greatly when the deposits thickness is varied. This is a consequence of the cubic term present in Equation (5). One can also notice that the mass flow calculated with Equation (5) is sensitive to the chosen angle.

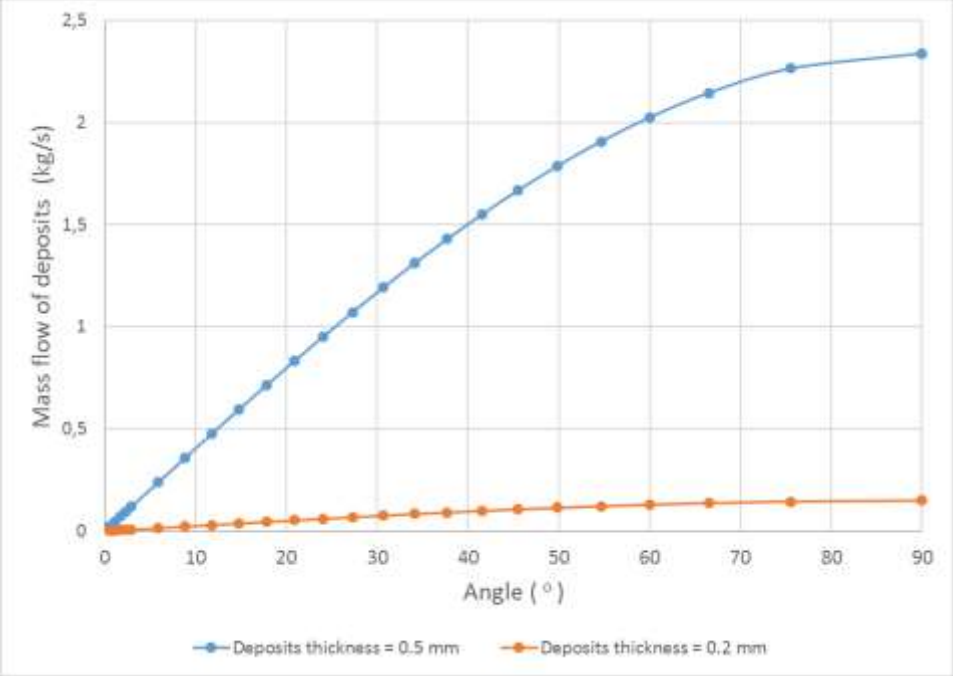

Figure 7. Calculated mass flow of deposits as function of angle via Equation (5) for two different deposits thickness (0.5 mm and 0.2 mm).

By using again Equation (5), but this time with values of mass flow (0.14 kg/s and 0.002 kg/s) reported in references [7, 19], L = 30 m, and the properties of Table 1, the deposits thickness is calculated for different angles (Figure 8). Results show that the deposits thickness is again

sensitive to its mass flow, but this time the effect of the angle, especially in the range below 10 °, is more significant. As shown in Equation (5), the angle, through the gravitational acceleration in the flow direction, is in the denominator part of a cubic root function. To exemplify this situation, a mass flow of 0.14 kg/s is chosen; the calculated deposits thickness is then 0.6 mm for an angle of 2° while its value falls to 0.3 mm for an angle of 20 °.

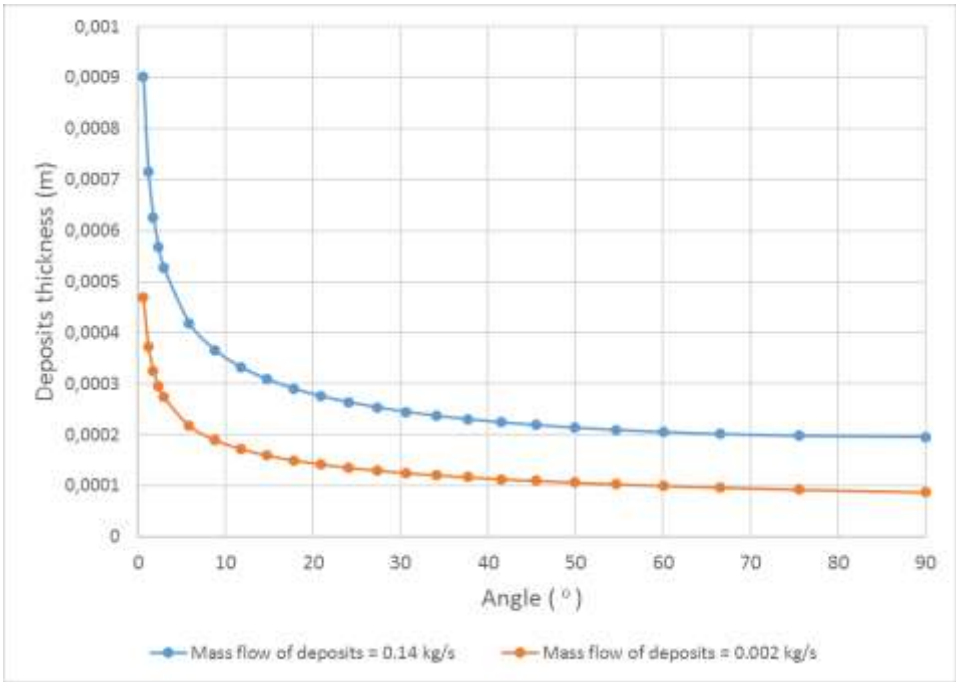

Figure 8. Calculated deposits thickness as function of angle via Equation (5) for two different mass flow of deposits (0.14 kg/s and 0.002 kg/s).

Table 4 compares the mass flow of deposits and the corresponding thickness reported in references [7, 19] to the values calculated with the proposed model. The time-varying mass flows presented in Figure 6 are converted into their root mean square (RMS) values using Equation (6), where n corresponds to the number of time steps. For the ease of presentation, only the results for x = 0.007 m are presented. For consistency, the deposits thicknesses calculated with Equation (5) in references [7, 19] are also reported (in parenthesis) for an angle of 20 °.

$$\dot{m} \qquad \sqrt{-\sum[\dot{m}(t_i)]} \tag{6}$$

Results from Table 4 show that the calculated mass flow of deposits is in the same range as the values reported in references [7, 19]. The deposits final thicknesses obtained with the model are equivalent to the results from Equation (5), especially if the angle of 20 ° is considered for which a value of 0.3 mm is obtained for a mass flow of 0.14 kg/s. As presented in Figure 8, the deposits thickness is sensitive to the chosen angle, thus the values of 0.7 mm and 0.2 mm reported in Table 4 are somewhat overestimated for an inclined plane of 20°. The results from Table 4 show the reliability of the present calculations when the steady-state is reached. Indeed, Equation (5) results from a force balance within a laminar flow in steady-state. For the same conditions, calculations from the current work are consistent with this force balance and thus with Newton 2nd law.

Table 4. Simulated mass flow and thickness of deposits, and comparison with the results reported in references [7, 18].

Reference	Mass flow of deposits (kg/s)	Initial thickness (mm)	Final thickness (mm)
[7]	0.14	0.70 (0.3*)	0.70 (0.3*)
[16]	0.002	0.20 (0.15*)	0.20 (0.15*)
Current work	0.027	0.5	0.25
Current work	0.13	1.5	0.40

* calculated with Equation (5) for an angle of 20 ^{o}.

From an industrial point of view, the approach presented in this paper is more realistic than the calculation using Equation (5), because it takes into account the effects of surface tension which, to author's knowledge, is essential in order to represent mathematically the mass flow of thin deposits. Moreover, the proposed model considers transient behavior, predicts the final deposits thickness, and it is applicable in a wide range of conditions (turbulent flow, wettability, nature of the cathode material). However, as reported in the assumptions, no metal movement from MHD effects nor heat transfer is considered in the present model. The authors are aware that these elements should be improved in order to add more realism the modeling of the deposits. A previous study concluded that the metal flow has a considerable impact on the bath film formation rate [9].

4. Concluding Remarks

A numerical model has been developed in order to understand more clearly the behavior of the deposits at the surface of the cathode. It consists of a transient multiphase finite-volume model coupling the mass and momentum conservation equations to a hybrid method combining the volume of fluid and level-set function. The numerical model enabled to predict the time-varying velocity field and volume fraction of the deposits. From these predictions, the mass flow of deposits moving along an inclined geometry, representing the cathodic slope on the sidewall, was calculated and compared to values reported in the open literature. The proposed model was finally used to verify the impact of the initial deposits thickness on their movement and estimate the corresponding mass flow. For a cathodic panel periphery of 30 m long, results showed that the mass flow of the deposits varied over time, with a rapid initial peak and an exponential decrease ending up to a value two orders of magnitude smaller than the peak. For an initial thickness of 0.5 mm and 1.5 mm, the calculated final thicknesses were respectively 0.25 mm and 0.4 mm, while the mass flow peak values were 0.17 - 0.19 kg/s and 0.55 - 0.76 kg/s.

The objective of the current work was to gain knowledge on the deposits mass transfer in the optics of later adjusting the operational parameters of the electrolysis cell or to modify the design of cathode blocks that minimize the resistive deposits on its surface. In order to achieve these significant modifications, more modeling work is currently underway. Results of these analyses will be reported in the near future. In this study, the proposed model remains preliminary in the sense that the complexity of the coupled phenomenon occurring at the surface of cathode blocks has been simplified to conduct the analysis with reasonable computer resources, which in hand affects the realism of the numerical model. Moreover, the *in situ* measurements of the deposits thickness on the surface of a cathode of an operating cell is challenging task, thus for the moment, these measurements are not available to feed the numerical model, making the modeling step even more difficult.

5. Acknowledgments

The authors are very grateful to the Natural Sciences and Engineering Council of Canada (NSERC) and to RioTinto for their financial support.

6. References

1. Jean-René Landry, Mojtaba Fallah Fini, Gervais Soucy, Martin Désilets, Patrick Pelletier, Loig Rivoaland, and Didier Lombard, Laboratory study of the impact of the cathode grade on the formation of deposits on the cathode surface in Hall-Héroult cells, *Light Metals* 2018, 1229-1233.
2. Marc-André Coulombe, Gervais Soucy, Loig Rivoaland, and Lynne Davies, Factors leading the formation of a resistive thin film at the bottom of aluminum electrolysis cells, *Metallurgical and Materials Transactions B*, Vol. 47, No. 2 (2016) 1280-1295.
3. Marc-André Coulombe, Gervais Soucy, Martin Désilets, and Didier Lombard, The effect of ledge toe and thin film formation on cathode voltage drop in aluminium electrolysis cells, *Canadian Metallurgical Quarterly*, Vol. 55, No. 3 (2016), 376-386.
4. Marc-André Coulombe, Étude de la formation et du comportement d'un dépôt de boue au centre de la cuve à l'interface cathodique, *PhD thesis*, Université de Sherbrooke, 2015,172 p.
5. François Allard, Gervais Soucy, and Loig Rivoaland, Formation of deposits on the cathode surface of aluminum electrolysis cells, *Metallurgical and Materials Transactions B*, Vol. 45, No. 6 (2014) 2475-2485.
6. François Allard, Marc-André Coulombe, Gervais Soucy, and Loig Rivoaland, Cartography and chemical composition of the different deposits in the Hall-Héroult process, *Light Metals* 2014, 1233-1238.
7. Asbjørn Solheim, Towards a proper understanding of sideledge facing metal in aluminum cells?, *Light Metals* 2006, 439-443.
8. Warren E. Haupin, Calculating thickness of containing walls frozen from melt, *Journal of Metals*, Vol. 23, No. 7 (1971) 41-44.
9. Nils-Håvard Giskeødegård, Asbjørn Solheim, and Nancy J. Holt, Sideledge facing metal in aluminum electrolysis cells: preliminary modelling study of bath film formation, *Light Metals* 2016, 423-428.
10. Marc Dupuis, Computation of aluminum reduction cell energy balance using ANSYS finite element models, *Light Metals* 1998, 409-417.
11. Øyvind Østrem, Cathode wear in Hall–Héroult cells, *Ph.D. Thesis,* Norwegian University of Science and Technology, 2013, 243 pages.
12. Bogdan A. Nichita, Iztok Zun, and John R. Thome, A level set method coupled with a volume of fluid method for modeling of gas-liquid interface in bubby flow, *Journal of Fluids Engineering*, Vol. 132, No. 8 (2010) 1-15.
13. ANSYS Fluent theory guide, Release 15.0, ANSYS Inc., Cannonsburg, PA, USA, 2013.
14. Mark Sussman, and Elbridge G. Puckett, A coupled level set and volume of fluid method for computing 3D and axisymmetric incompressible two-phase flows, *Journal of Computational Physics*, Vol. 162, No. 2 (2000) 301-337.
15. Joshua Blake, David Thompson, Dominik Raps, and Tobias Strobl, Simulating the freezing of supercooled water droplets impacting a cooled substrate, *AIAA Journal*, Vol. 53, No. 7 (2015) 1725-1739.
16. Christopher W. Bale et al., FactSage thermochemical software and databases, 2010-2016, *Calphad*, Vol. 54 (2016) 35-53.
17. Jeremiah U. Brackbill, Douglas B. Kothe, and C. Zemach, A continuum method for modeling surface tension, *Journal of Computational Physics,* vol. 100 (1992) 335-354.
18. Michal Korenko, Interfacial tension between aluminum and cryolite alumina melts, *Journal of Chemical Engineering Data*, Vol. 53, No. 3(2008) 794-797.
19. Knut Tørklep et al., Alumina distribution in point-fed Hall-Héroult cells, *Light Metals* 1997, 377-386.